Studies of the New Herbicide KIH-6127. 4. Crystal Structure of KIH-6127 and Quantitative Structure−Activity Relationship of the Iminoxy Moiety of KIH-6127 Derivatives

Masatoshi Tamaru,*,† Jun Inoue,† Ryo Hanai,‡ and Shigehiko Tachikawa‡

KI Chemical Research Institute Co., Ltd. Shioshinden 478-1, Fukude-cho, Iwata-gun, Shizuoka 437-12, Japan, and Kumiai Chemical Industry Co., Ltd., Life Science Research Institute, Kikugawa, Ogasa-gun, Shizuoka 439, Japan

The crystal structure of the major isomer of KIH-6127 was investigated by X-ray crystallographic techniques. The solid state structure and its conformation were confirmed as the *E* form. Thus KIH-6127 is mainly consistent with methyl 2-[(4,6-dimethoxypyrimidin-2-yl)oxy]-6-[1-*E*-(methoxyimino)ethyl] benzoate (compound **1**: Table 1). Further modifications of the iminoxy moiety to introduce a variety of haloalkyl, haloalkenyl, and others were made, and the *Z* isomers of several derivatives were prepared. The physicochemical properties of these derivatives were measured, including their log *P* and K_d values. We tested their herbicidal activity against barnyard grass and their phytotoxicity to transplanted rice in flooded paddy conditions. We also studied the role of the iminoxy moiety, on the basis of the hypothesis that the difference in the *E*/*Z* configurations of the iminoxy moiety determines their biological activity. However, clear differences in the herbicidal activities were not observed between these isomer groups. Each *Z* isomer was more hydrophilic than its *E* counterpart. To investigate this finding more intensively in a single *E*/*Z* pair, the surface area of each *E*/*Z* isomer of KIH-6127 was calculated from the X-ray data for the KIH-6127 *E* form. The *Z* conformation of the iminoxy moiety appears to take a more compact molecular conformation, resulting in the *Z* isomer having more hydrophilic surface area than the corresponding *E* isomer. QSAR studies focused on the iminoxy moiety. Both pre- and post-emergence activities of the compounds were well correlated with the square of the log *P* value for both configurations of the iminoxy moiety. In other words, these configurations merely contributed to the activity by way of their hydrophilicity. The difference between optimum log *P* values for pre- versus post-emergence indicated that the optimum compound is more lipophilic for pre- than for post-emergence activity. Phytotoxity against rice also correlated well with the K_d value. Thus stronger soil adsorption of the compounds provides higher safety for rice. On the basis of those QSAR studies, compound **1** was selected as the optimal compound for development as a commercial herbicide.

Keywords: *Methyl 2-[(4,6-dimethoxypyrimidin-2-yl)oxy]-6-[1-E-(methoxyimino)ethyl] benzoate; KIH-6127; Pyriminobac-methyl; herbicide; barnyard grass; ALS; QSAR*

INTRODUCTION

Methyl 2-[(4,6-dimethoxypyrimidin-2-yl)oxy]-6-[1-(methoxyimino)ethyl] benzoate [KIH-6127, Pyriminobac-methyl; Figure 1, **1**; the technical grade is a mixture of the *E* and *Z* forms (**2**), respectively] has been found to be particularly effective herbicide against barnyard grass (*Echinochloa oryzicola*) over a wide range of growth stages including pre-emergence application. This compound has excellent safety for transplanted rice crops in flooded paddy conditions (Hanai *et al*., 1993). Pyriminobac-methyl was approved in 1996 and was first launched earlier this year as one of the active ingredients of the one-shot rice herbicide Prosper (trade name of Kumiai) in Japan. Compound **1** has been proposed to inhibit the plant enzyme acetolactate synthase (ALS), blocking branched chain amino acid biosynthesis (Shimizu *et al*., 1994).

As reported previously (Tamaru *et al*., 1997), synthesis of KIH-6127 yields a mixture of two isomers (**1** and **2**) in a >9:1 (major/minor) ratio. These isomers have been separated by silica-gel column chromatography, and their stereochemistry was initially determined by NMR spectrometry. The major isomer was tentatively assigned as being the *E* isomer (**1**) (Tamaru *et al*., 1997). However, we required more precise structural information for compound **1** for our project. In this paper, we report results of X-ray crystallography to determine the solid state structure and precise configuration of the 1-(methoxyimino)ethyl moiety of compound **1**.

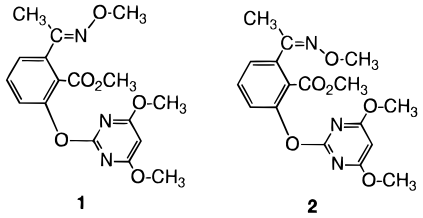

Figure 1. KIH-6127 (**1**) and its *E* form (**2**).

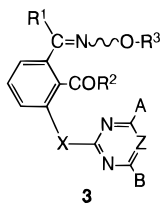

Figure 2. General structure of KIH-6127 analogues (**3**).

* Author to whom correspondence should be addressed.

† KI Chemical Research Institute Co., Ltd.

‡ Kumiai Chemical Industry Co., Ltd.

S0021-8561(96)00844-8 CCC: $14.00 © 1997 American Chemical Society

Table 1. Herbicidal Activities and Physicochemical Properties of Test Compounds

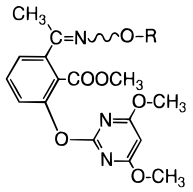

compd no.	R	*Ec*.Pre[a] pI_{50} (mol ai a^{-1})	*Ec*.Pre[a] ED_{50} (g ai a^{-1})	*Ec*.Pre[a] calcd[b] eq 1	*Ec*.Pre[a] calcd[b] eq 2	*Ec*.3L[c] pI_{50} (mol ai a^{-1})	*Ec*.3L[c] ED_{50} (g ai ha^{-1})	*Ec*.3L[c] calcd eq 3	*Or*[d] pI_{50} (mol ai a^{-1})	*Or*[d] ED_{50} (kg ai ha^{-1})	*Or*[d] calcd eq 4	physicochemical properties log P[e]	physicochemical properties K_d[f]
1	OMe (*E*)	4.16	2.50	4.18	4.16	3.83	5.34	3.79	1.85	0.51	1.84	2.57	0.899
2	OMe (*Z*)	3.78	6.00	(3.94)	3.92	3.66	7.90	3.65	1.87	0.49	1.94	2.11	0.625
4	OEt (*E*)	4.18	2.48	4.25	4.24	3.67	8.02	3.77	1.78	0.62	1.77	2.96	1.070
5	OEt (*Z*)	4.18	2.48	(4.14)	4.13	3.74	6.82	3.78	1.70	0.74	1.76	2.49	1.100
6	OPr (*E*)	4.19	2.51	4.15	4.15	3.54	11.23	3.46	1.62	0.93	1.56	3.59	1.640
7	OPr (*Z*)	4.25	2.19	(4.26)	4.25	3.90	4.90	3.75	1.82	0.59	1.70	3.01	1.270
8	OCH_2CH_2Cl (*E*)	4.21	2.52	4.24	4.24	3.56	11.26	3.68	1.44	1.49	1.48	3.23	1.870
9	OCH_2CH_2Cl (*Z*)	4.21	2.52	(4.24)	4.23	3.90	5.15	3.79	1.55	1.16	1.64	2.85	1.430
10	$OCH_2CH{=}CH_2$ (*E*)	4.20	2.44	4.25	4.24	3.73	7.21	3.71	1.59	1.00	1.62	3.13	1.490
11	$OCH_2CH{=}CH_2$ (*Z*)	4.20	2.44	(4.22)	4.20	3.80	6.14	3.80	1.83	0.57	1.73	2.74	1.200
12	OBu	3.78	6.69	3.86	3.86	3.03	37.65	2.96	NT[g]	NT		4.11	NT
13	OCH_2CH_2F	4.14	2.85	4.06	4.04	NT	NT		NT	NT		2.31	NT
14	OCH_2CF_3	4.23	2.53	4.21	4.21	NT	NT		NT	NT		3.39	NT
15	$OCH_2CH{=}CCl_2$	3.81	7.07	3.76	3.76	NT	NT		NT	NT		4.23	NT
16	OH	3.73	6.47	3.82	3.79	3.50	10.98	3.55	NT	NT		1.93	NT
17	OAc	3.65	8.72	3.60	3.56	3.38	16.23	3.36	NT	NT		1.68	NT
18	$OCH_2C[Cl]{=}CH_2$	4.28	2.21	4.13	4.13	3.42	16.04	3.43	1.63	0.99	1.62	3.63	1.490
19	$OCH_2C[Br]{=}CH_2$	4.15	3.30	4.09	4.09	3.19	30.11	3.35	1.43	1.73	1.45	3.73	1.940
20	OCH_2Ph	3.82	6.62	3.92	3.92	NT	NT		NT	NT		4.01	NT

[a] Herbicidal activity against *E. oryzicola* in pre-emergence. [b] Calculated by the QSAR equations. [c] Herbicidal activity against *E. oryzicola* in three-leaf growth stage. [d] Phytotoxity against *O. sativa*. [e] Logarithm of partition coefficient in 1-octanol/water. [f] The K_d value as soil adsorption. [g] NT, not tested.

Structure−activity studies examined the influences of the following moieties on biological activity: 6-alkyl (R^1), ester (R^2), alkoxyimino (R^3), the bridge atom (X), and the 4,6-disubstituted pyrimidine moieties (A, B, Z) (Figure 2, compound **3**) (Tamaru *et al*., 1997). The results showed that the iminoxy moiety has the dominant effects on biological activity. Changes of the alkyl group in the iminoxy moiety were less influential on biological activity. Thus, changes in the iminoxy moiety offered the most structural flexibility without adversely affecting biological activity.

To investigate the contribution of iminoxy moiety, the QSAR study focused on the iminoxy derivatives including the *Z* isomers and clarified physicochemical and stereochemical behavior on biological activities.

MATERIALS AND METHODS

Preparation of Test Compounds. Physical properties of test compounds covered in this paper are given in Table 2. Melting points cited are not corrected. The structures of the compounds were confirmed by NMR along with IR and mass spectroscopy. ^{1}H NMR spectra were obtained on a JEOL JMN-PMX-60si. The solvent used was deuterochloroform unless otherwise noted. ^{1}H chemical shifts are in parts per million (δ) with respect to tetramethylsilane. Test compounds (Figure 2, structure **3**; also see Tables 1 and 2) were synthesized according to the procedure previously reported (Tamaru *et al*., 1996, 1997) except compound **16** (Figure 3). The *Z* isomers were separated and purified by silica-gel column chromatography or high-pressure liquid chromatography (HPLC) as reported (Tamaru *et al*., 1997). HPLC was carried out on a JASCO, PU-981/UV-970 with following conditions: the column (octadecylsilica, particle size 120 Å) was 4.6 × 150 mm (AM-302, YMC); solvent system was acetonitrile/water = 6/4 (v/v) (sensitivity, 0.02 AuFS); flow rate, 1 mL/min; column temperature, 35 °C; UV detection, at 245 nm; injection volume, 10 μL). Unless otherwise noted, the inorganic chemicals and reagent grade solvents were obtained from Wako and Cica, and the organic reagents were from Aldrich and Wako. The water used for HPLC was obtained from Milli-RX and Milli-Q systems.

Synthesis of Compounds 16 and 23. Among all test compounds, compound **16** (Figure 3 and Table 1) was obtained in lower yield (12.5%) along with the undesired **23** (Figure 3) due to further cyclization of **16**. This synthesis used potassium acetate base in methanol at reflux for 1 h or at room temperature overnight (Tamaru *et al*., 1997). The amount of **23** gradually increased, depending on the reaction time, despite the presence of unreacted starting material, **21** (Figure 3). Improvement was necessary because **16** was used as the starting material for synthesis of other derivatives.

We initially proposed that such cyclization reactions may be enhanced under base conditions or higher reaction temperatures. However, treatment of **21** without potassium acetate still gave unacceptable formation of **23**. After several attempts, we found that some experimental runs without the drying tube gave relatively good yields. Thus the reaction using aqueous hydroxylamine hydrochloride (**22**) at 5 °C gave desired **16** in good yield (63%).

Synthesis of Methyl 2-[(4,6-Dimethoxypyrimidin-2-yl)-oxy]-6-[1-(hydroxyimino)ethyl] Benzoate (16). An aqueous solution of hydroxylamine hydrochloride (**22**: 19.7 g, 0.275 mol, in 45 mL of water) was added dropwise to a solution of methyl 2-acetyl-6-[(4,6-dimethoxypyrimidin-2-yl)oxy] benzoate (**21**: 8.3 g, 0.25 mol) in methanol (550 mL) at 5 °C. The mixture was stirred overnight at 5 °C and then poured into cold water and extracted with ethyl acetate. The organic layer was washed with water, dried over anhydrous magnesium sulfate, and concentrated *in vacuo* at 25 °C. The residue was dissolved in a small amount of ethyl acetate and purified by silica-gel column chromatography with hexane + ethyl acetate (10+1 to 6+1 by volume) as the eluent to give **16** (5.5 g; 63% yield). NMR chemical shifts and melting points are cited in Table 2.

Selective Synthesis of 8-[(4,6-Dimethoxypyrimidin-2-yl)oxy]-4-methylbenzo[*d*]oxazin-1-one (23). A suspension of **21** (15.1 g, 0.0454 mol) and **23** (4.74 g, 0.0681 mol) in methanol (200 mL) was refluxed with stirring for 2 h until

Table 2. Physicochemical Properties and NMR Data for Compounds 1−20

compd no.	mp (°C)	n_D^{20}	[^{1}H]NMR δ (ppm)
1	106−107		2.17 (s, 3H), 3.76 (s, 3H), 3.82 (s, 6H), 3.96 (s, 3H), 5.73 (s, 1H), 7.16−7.50 (m, 3H)
2	59−60		2.20 (s, 3H), 3.65 (s, 3H), 3.69 (s, 3H), 3.83 (s, 6H), 5.73 (s, 1H), 6.90−7.70 (m, 3H)
4	93−95		1.26 (t, J = 7 Hz, 3H), 2.17 (s, 3H), 3.79 (s, 3H), 3.83 (s, 6H), 4.23 (q, J = 7 Hz, 2H), 5.73 (s, 1H), 7.00−7.67 (m, 3H)
5	68−70		1.07 (t, J = 6 Hz, 3H), 2.20 (s, 3H), 3.57 (s, 3H), 3.76 (s, 6H), 3.97 (q, J = 6 Hz, 2H), 5.70 (s, 1H), 6.85−7.67 (m, 3H)
6	73−76		1.00 (t, J = 7 Hz, 3H), 1.70 (q, J = 7 Hz, 2H), 2.23 (s, 3H), 3.73 (s, 3H), 3.83 (s, 6H), 4.13 (t, J = 7 Hz, 2H), 5.73 (s, 1H), 7.00−7.83 (m, 3H)
7	NM		0.83 (t, J = 7 Hz, 3H), 1.57 (q, J = 7 Hz, 2H), 2.20 (s, 3H), 3.53 (s, 3H), 3.73 (s, 6H), 3.83 (t, J = 7 Hz, 2H), 5.72 (s, 1H), 6.92−7.67 (m, 3H)
8		1.5540	2.20 (s, 3H), 3.75 (s, 3H), 3.80 (s, 6H), 3.50−4.0 (m, 2H), 4.34 (t, J = 6 Hz, 2H), 5.80 (s, 1H), 7.16−7.67 (m, 3H)
9	NM[a]		2.23 (s, 3H), 3.60 (t, J = 6 Hz, 2H), 3.60 (s, 3H), 3.77 (s, 6H), 4.13 (t, J = 6 Hz, 2H), 5.73 (s, 1H), 6.85−7.70 (m, 3H)
10	76−78		2.20 (s, 3H), 3.66 (s, 3H), 3.79 (s, 6H), 4.60 (q, J = 6 Hz, J = 2 Hz, 2H), 5.0−5.15 (m, 1H), 5.30 (q, J = 10 Hz, J = 2 Hz, 1H), 5.69 (s, 1H), 5.75−6.15 (m, 1H), 7.00−7.50 (m, 3H)
11	NM		2.17 (s, 3H), 3.53 (s, 3H), 3.70 (s, 6H), 4.33 (q, J = 8 Hz, J = 2 Hz, 2H), 4.90−5.05 (m, 1H), 5.20 (q, J = 10 Hz, J = 2 Hz, 1H), 5.72 (s, 1H), 5.53−6.23 (m, 3H), 6.89−7.65 (m, 3H)
12		1.5374	0.8−2.2, (m, 7H), 2.45 (s, 3H), 4.10 (s, 3H), 4.25 (s, 6H), 4.65 (t, J = 5 Hz, 2H), 6.35 (s, 1H), 7.7−8.1 (m, 3H)
13	90−92		2.20 (s, 3H), 3.38 (s, 3H), 3.50 (s, 6H), 3.50−4.17 (m, 2H), 4.20−4.50 (m, 2H), 4.67−5.00 (m, 2H), 5.50 (s, 1H), 6.85−7.50 (m, 3H)
14	63−64		2.00 (s, 3H), 3.43 (s, 3H), 3.57 (s, 6H), 4.30 (q, J = 8 Hz, J = 18 Hz), 5.50 (s, 1H), 6.83−7.50 (m, 3H)
15		1.5579	2.25 (s, 3H), 3.79 (s, 3H), 3.83 (s, 6H), 4.69 (t, J = 8 Hz), 5.83 (s, 1H), 6.00−6.40 (m, 1H), 7.15−7.85 (m, 3H)
16	131−132		2.15 (s, 3H), 3.66 (s, 3H), 3.76 (s, 6H), 5.69 (s, 1H), 7.03−7.66 (m, 3H), 9.00 (broad, 1H)
17		1.5510	2.16 (s, 3H), 2.26 (s, 3H), 3.66 (s, 3H), 3.76 (s, 6H), 5.73 (s, 1H), 7.080−7.73 (m, 3H)
18	54−56		2.30 (s, 3H), 3.77 (s, 3H), 3.87 (s, 6H), 4.75 (s, 1H), 5.40−5.63 (m, 1H), 5.83 (s, 1H), 7.16−7.84 (m, 3H)
19		1.5576	2.16 (s, 3H), 3.67 (s, 3H), 3.87 (s, 6H), 4.73 (s, 2H), 5.77 (s, 1H), 5.57−6.00 (m, 2H), 7.15−7.73 (m, 3H)
20		1.5689	2.16 (s, 3H), 3.53 (s, 3H), 3.63 (s, 6H), 5.10 (s, 2H), 5.67 (s, 1H), 6.83−7.83 (m, 8H)

[a] NM, not measured due to viscous oil.

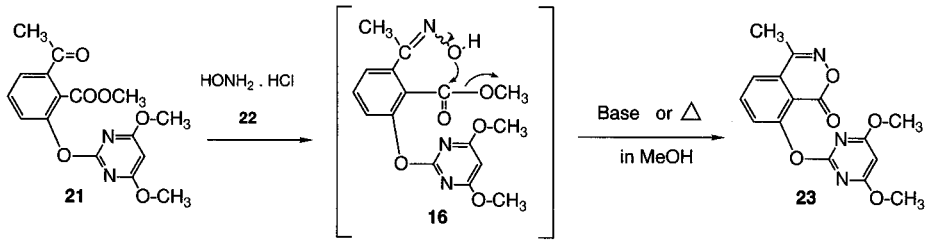

Figure 3. Synthesis of **16** and further cyclization reaction of **16**.

dissolved. During additional heating for 8 h, a white precipitate was gradually observed in the reaction solvent. The reaction mixture was then cooled to room temperature, and the precipitate was filtered and washed with isopropyl ether to give **23** (6.5 g; 45.4% yield); mp 168−170 °C. [^{1}H]NMR δ: 2.53 (s, 1H), 3.73 (s, 1H), 5.70 (s, 1H), 7.40−8.07 (m, 3H) ppm.

Formulation of Test Chemicals and Preparation of Test Pots. Each test compound was formulated as a 100 g ai/kg wettable powder, containing Emalgen 810 (5.0 g kg^{-1}, 1-octyl-4-polyoxoethyleneoxybenzene, Kao Ltd.), Demolon (5.0 g kg^{-1}, sodium polymethylnaphthalenesulfonic acid, Kao Ltd.), Kunilite 250 (180 g kg^{-1}, diatomaceous earth, Kunimine Ltd.), Carplex No. 80 (60 g kg^{-1}, silicon dioxide, Shionogi Co., Ltd.), and Zeeklite (clay).

The wettable powder was diluted with water to the desired concentrations. Plastic pots (square; 100 cm^2 in surface area) were filled with paddy soil (clay loam soil: sand 45%, silt 31.1%, and clay 23.9%; organic matter 1.44%, pH 5.6), which was collected locally from a paddy field in Kikugawa, Japan. Unless otherwise noted, the same soil was used in this work. Water was added up to 3 cm in depth to create flooded paddy conditions. The level of flooding water was maintained throughout the test period. Twenty seeds of *E. oryzicola* (*Ec*) were seeded at a depth of 0.5 cm one day after puddling and fertilization. A rice seeding (*Oryza sativa*, two-leaf growth stage) (*Or*) was transplanted at a depth of 3 cm in the same pot. One day after seeding for the pre-emergence test or when *Ec* reached the three-leaf growth stage for the post-emergence test, an aqueous solution (10 mL) of a wettable powder of the chemicals at the desired dosages was shaken and poured into the pots individually. The test pots were placed in a greenhouse and maintained under the following conditions throughout the experiments: room temperature was maintained at 20−35 °C and water temperature was maintained at 15−30 °C, under natural daylight conditions.

Evaluation of Biological Activities. The herbicidal symptoms of all test compounds were the same: stunting and slight yellowing. These symptoms are typical for ALS inhibitors (Shimizu *et al*., 1994). The results of the visual evaluation scores based on these symptoms are well correlated empirically to those based on dry weights. Therefore, we used an empirical visual evaluation method focusing on the stunting symptom. Three weeks after treatment (DAT 21), the herbicidal activity and rice injury ratings were visually evaluated on a percent scale, comparing the herbicidal symptoms of each observed pot with two reference pots which indicated 0% (= no control or no crop injury) and 100% (= completely killed). ED_{50} values were calculated as the amounts of active ingredient per hectare (g ai ha^{-1}) required for 50% of maximum injury to barnyard grass or rice. For the QSAR analysis, the activity of each chemical against barnyard grass and rice is expressed as I_{50} (I_{50} = ED_{50}/[MW × 10^2]), i.e., units of molar concentration of active ingredient per are (M ai a^{-1}). QSAR equations were carried out using pI_{50} (log[1/I_{50}]; the logarithm of the reciprocal of I_{50}). These biological activities (ED_{50}(*Ec*) in g ai ha^{-1}, ED_{50}-(*Or*) in kg ai ha^{-1}, and pI_{50} in mol ai a^{-1}) are cited in Table 1.

Table 3. Atomic Positional and Equivalent Isotropic Thermal Parameters of KIH-6127 *E* Form[a]

atom	*x*	*y*	*z*	B_{iso}/B_{eq} (Å)^2	atom	*x*	*y*	*z*	B_{iso}/B_{eq} (Å)^2
O(1)	0.2744(1)	−0.1206(2)	0.2012(1)	0.2012(1)	C(15)	0.1099(2)	0.2708(3)	0.1478(1)	3.54(6)
O(2)	0.2551(1)	0.0280(2)	0.0810(1)	4.39(5)	C(16)	0.0508(2)	0.4085(4)	0.1012(2)	5.30(8)
O(3)	0.4375(1)	0.0999(2)	0.2697(1)	3.94(5)	C(17)	−0.0302(3)	−0.0872(5)	0.1094(2)	6.85(10)
O(4)	0.3243(1)	−0.0794(2)	0.5032(1)	4.46(5)	H(3)	0.4518	0.4166	0.3348	4.2000
O(5)	0.5782(1)	−0.3633(2)	0.4044(1)	4.37(5)	H(4)	0.3294	0.6284	0.3078	4.4000
O(6)	−0.0085(1)	0.0880(3)	0.1061(1)	5.91(6)	H(5)	0.1705	0.5543	0.2261	4.1000
N(1)	0.3811(1)	0.0112(2)	0.3893(1)	3.29(5)	H(8a)	0.2306	−0.1052	−0.0223	5.8000
N(2)	0.5084(1)	−0.1275(2)	0.3358(1)	3.41(5)	H(8b)	0.1782	−0.1920	0.0502	5.8000
N(3)	0.0832(1)	0.1175(3)	0.1515(1)	4.18(6)	H(8c)	0.2964	−0.2014	0.0489	5.8000
C(1)	0.2784(2)	0.1823(3)	0.2073(1)	3.00(6)	H(11)	0.4639	−0.3228	0.5109	3.4000
C(2)	0.3640(2)	0.2219(3)	0.2589(2)	3.45(6)	H(13a)	0.3060	−0.3003	0.5458	5.6000
C(3)	0.3839(2)	0.3807(3)	0.2934(2)	4.28(7)	H(13b)	0.2545	−0.3003	0.5458	5.6000
C(4)	0.3143(2)	0.5071(3)	0.2776(2)	4.50(7)	H(13c)	0.3836	−0.2255	0.6135	5.6000
C(5)	0.2267(2)	0.4694(3)	0.2294(2)	4.19(7)	H(14a)	0.6110	−0.3740	0.2880	5.0000
C(6)	0.2064(2)	0.3078(3)	0.1943(1)	3.28(6)	H(14b)	0.6914	−0.4600	0.3598	5.0000
C(7)	0.2676(2)	0.0132(3)	0.1650(2)	3.52(7)	H(14c)	0.6820	−0.2346	0.3510	5.0000
C(8)	0.2380(3)	−0.1295(4)	0.0339(2)	5.94(8)	H(16a)	0.0926	0.5004	0.0672	5.2000
C(9)	0.4409(2)	−0.0100(3)	0.3358(1)	3.22(6)	H(16b)	−0.0010	0.3707	0.0564	5.2000
C(10)	0.3882(2)	−0.1058(3)	0.4518(2)	3.32(6)	H(16c)	0.0325	0.4824	0.1345	5.2000
C(11)	0.4534(2)	−0.2377(3)	0.4593(1)	3.49(6)	H(17a)	−0.0205	−0.1337	0.1544	6.7000
C(12)	0.5131(2)	−0.2399(3)	0.3986(2)	3.35(6)	H(17b)	−0.0994	−0.1144	0.0655	6.7000
C(13)	0.3159(2)	−0.2090(4)	0.5666(2)	5.74(8)	H(17c)	0.0255	−0.1884	0.0824	6.7000
C(14)	0.6447(2)	−0.3601(4)	0.3444(2)	5.11(8)					

[a] Estimated standard deviations in parentheses.

Structure−Activity Studies. The structure−activity correlation was analyzed by multiple regression analysis (Fujita *et al.*, 1964), using the TUTORS program (Takahashi *et al.*, 1989). The regression was done stepwise, introducing or withdrawing parameters to minimize the sum of squared deviations. The level of significance of each term was judged by the *F*-ratio and Student's *t*-tests.

In our preliminary analysis employing several substituent parameters (i.e., Hansch−Fujita's substituent parameter, π, and the electronic parameter, σ, etc.), an indicator variable which represents *E*/*Z* configurations was also considered as a descriptor, due to the difficulty of discriminating such stereochemistry by substituent parameter (i.e., each *E*/*Z* isomeric substituent pair has the same π value). All attempts using such substituent parameters did not gave satisfactory results. Finally we selected the log *P* (1-octanol/water partition coefficient) and K_d (soil adsorption coefficient) values (Lambert *et al.*, 1968) which represent the full molecule and which were obtained experimentally.

Measurements of the log *P* and K_d Values. The log *P* and K_d values are listed in Table 1. The log *P* values used in this study were obtained experimentally by the shake-flask method (Fujita *et al.*, 1964; OECD, 1989). Soil adsorption coefficients were obtained experimentally as follows: Kikugawa soil (used in biological tests also and described under Preparation of Test Pots) was sieved under 0.5 mm after drying at 80 °C for 24 h and then at 120 °C for 24 h at 30 mmHg. The soil (6 g, dry weight), with 30 mL of aqueous $CaCl_2$ (10^{-2} M) solution containing the test compound at four different concentrations (water solubility (WS) > 10 ppm and compound at 5, 2.5, 1.25, and 0.625 ppm or WS < 10 ppm and compound at 0.5WS, 0.25WS, 0.125WS, and 0.0625WS), was shaken at 20 °C for 16−20 h. After being shaken, each suspension was centrifuged (8000 rpm for 20 min) and the concentration of the compound in the equilibrium solution was measured by HPLC (same conditions described in "Preparation of Test Compounds"). The amount of the compound adsorbed by the soil was obtained from measured concentrations of both the initial and equilibrium solutions.

The soil adsorption coefficient (K_d) and adsorption exponent (1/*n*) were obtained with the following equation:

$$\log x/m = \log K_d + 1/n \log C_w$$

where x/m is the equilibrium concentration of amounts of the compound adsorbed by a unit amount of soil (mg/g), which is equal to [amount of initially added test compound − amount of test compound in the equilibrium solution]/soil weight, and C_w is the equilibrium concentration of test compound in the solution phase (mg/mL).

X-ray Crystallography. Methyl 2-[1-(methoxyimino)-ethyl]-6-[(4,6-dimethoxypyrimidin-2-yl)oxy] benzoate (**1** and **2** as *E*/*Z* mixture in Figure 1) was prepared according to the procedure previously reported (Tamaru *et al.*, 1997). The major isomer, tentatively assumed as *E* isomer (**1**), was obtained by recrystallization from a mixture of ethyl acetate and diisopropyl ether. A colorless prism, single crystal of approximately 0.2 × 0.2 × 0.3 mm^3, was crystallized in the space group $P2_{1/a}$ (No. 14), with a = 14.2100 Å (2), b = 7.8590 Å (1), c = 15.9200 Å (2), β = 99.4400 Å (1), Z = 4, D_{calcd} = 1.368 g cm^{-3}, F_{000} = 760.00, and μ(CuKα) = 8.88 cm^{-1}, as monoclinic.

Data collection was performed with an automated diffractometer at room temperature. The number of reflections used for unit cell determination was measured within 2θ = (0.0−0.0°), with the graphite-monochromated CuKα radiation (I = 1.54178 Å). The R_{sym} of averaging the equivalent reflections was 0.018. The Omega scan peak width at half-height is 0.00°.

The structure was solved and resolved by the automatic structure analysis package for the microcomputer, based on MULTAN 78 (Main *et al.*, 1978). The structure was refined by the least squares method. The final *R* factor (the final agreement value) was 0.068, including hydrogen atoms.

Computation of Surface Area. The atomic coordinates of the *E* isomer determined by X-ray crystallography were transformed to the Cartesian coordinates to construct initial atomic coordinates for the computer graphics program. This conformation was used to calculate both MO (Dewar *et al.*, 1985) and surface area (Camilleri *et al.*, 1988).

Unfortunately, recrystallization of the *Z* isomer suitable for the analysis was unsuccessful due to its lower melting point (melting point of compound **2** is 59−60 °C; see Table 2). Therefore, the initial coordinates of the *Z* isomer were calculated by the following method: The methyl group at the imino moiety of the *E* isomer (compound **1**) was rotated to build *Z* form temporarily and the optimization of three-dimensional structure of both *E*/*Z* isomers was calculated by semiempirical quantum chemical calculations with the AM1 Hamiltonian of the MOPAC program (Dewar *et al.*, 1985). The surface areas of both *E*/*Z* isomers were calculated using the QCPE 413 program. The surface area, final heat of formulation (ΔH_f), and total energy are listed in Table 7.

RESULTS AND DISCUSSION

X-ray Crystallography. The final positional and thermal parameters for KIH-6127 *E* form (compound **1**) with their estimated standard deviations are listed in Table 3. The calculated bond lengths, bond angles,

Table 4. Bond Lengths (Å)

atom−atom	distance	atom−atom	distance
O(1)−C(7)	1.195(3)	C(6)−C(15)	1.477(4)
O(2)−C(7)	1.325(3)	C(10)−C(11)	1.383(3)
O(2)−C(8)	1.446(4)	C(11)−C(12)	1.386(3)
O(3)−C(2)	1.408(3)	C(15)−C(16)	1.490(4)
O(3)−C(9)	1.355(3)	C(3)−H(3)	1.110
O(4)−C(10)	1.334(3)	C(4)−H(4)	1.070
O(4)−C(13)	1.453(3)	C(5)−H(5)	1.030
O(5)−C(12)	1.333(3)	C(8)−H(8a)	0.900
O(5)−C(14)	1.450(3)	C(8)−H(8b)	1.050
O(6)−N(3)	1.402(3)	C(8)−H(8c)	1.000
O(6)−C(17)	1.414(4)	C(11)−H(11)	1.050
N(1)−C(9)	1.309(3)	C(13)−H(13a)	0.790
N(1)−C(10)	1.346(3)	C(13)−H(13b)	1.040
N(2)−C(9)	1.331(3)	C(13)−H(13c)	1.120
N(2)−C(12)	1.328(3)	C(14)−H(14a)	0.950
N(3)−C(15)	1.267(3)	C(14)−H(14b)	1.030
C(1)−C(2)	1.386(4)	C(14)−H(14c)	1.120
C(1)−C(6)	1.412(3)	C(16)−H(16a)	1.130
C(1)−C(7)	1.487(3)	C(16)−H(16b)	0.980
C(2)−C(3)	1.375(4)	C(17)−H(17a)	0.800
C(3)−C(4)	1.396(4)	C(17)−H(17b)	1.130
C(4)−C(5)	1.383(4)	C(17)−H(17c)	1.250
C(5)−C(6)	1.398(3)		

Table 5. Bond Angles (Deg)

atom−atom−atom	angle	atom−atom−atom	angle
O(7)−O(2)−C(8)	115.5(2)	C(4)−C(3)−H(3)	116.6
C(2)−O(3)−C(9)	117.4(2)	C(5)−C(4)−H(4)	117.8
C(10)−O(4)−C(13)	117.3(2)	C(5)−C(4)−H(4)	122.4
C(12)−O(5)−C(14)	117.5(2)	C(4)−C(5)−H(5)	120.4
N(3)−O(6)−C(17)	109.4(2)	C(6)−C(5)−H(5)	117.3
C(9)−N(1)−C(10)	114.6(2)	O(2)−C(8)−H(8a)	108.3
C(9)−N(2)−C(12)	114.1(2)	O(2)−C(8)−H(8b)	110.3
O(6)−N(3)−C(15)	113.1(2)	O(2)−C(8)−H(8c)	107.3
C(2)−C(1)−O(6)	118.3(2)	H(8a)−C(8)−H(8b)	112.0
C(2)−C(1)−C(7)	119.0(2)	H(8a)−C(8)−H(8c)	108.3
C(6)−C(1)−C(7)	122.7(2)	H(8b)−C(8)−H(8c)	110.5
O(3)−C(2)−C(1)	118.8(2)	C(10)−C(11)−H(11)	123.5
O(3)−C(2)−C(3)	118.0(2)	C(12)−C(11)−H(11)	120.9
C(1)−C(2)−C(3)	122.9(2)	O(4)−C(13)−H(13a)	111.9
C(2)−C(2)−C(12)	118.7(2)	O(4)−C(13)−H(13b)	104.2
C(3)−C(4)−C(5)	119.6(2)	O(4)−C(13)−H(13c)	112.6
C(4)−C(5)−C(6)	121.6(2)	H(13a)−C(13)−H(13b)	106.5
C(1)−C(6)−C(5)	118.6(2)	H(13a)−C(13)−H(13c)	104.2
C(1)−C(6)−C(15)	121.8(2)	H(13b)−C(13)−H(13c)	117.5
C(5)−C(6)−C(15)	119.5(2)	O(5)−C(14)−H(14c)	107.6
O(1)−C(7)−O(2)	123.5(2)	O(5)−C(14)−H(14a)	109.8
O(1)−C(7)−C(1)	125.0(2)	O(5)−C(14)−H(14b)	107.0
O(2)−C(7)−C(1)	111.5(2)	H(14c)−C(14)−H(14a)	110.4
O(3)−C(9)−N(1)	118.7(2)	H(14c)−C(14)−H(14b)	111.9
O(3)−C(9)−N(2)	112.1(2)	H(14a)−C(14)−H(14b)	110.0
N(1)−C(9)−N(2)	129.2(2)	C(15)−C(16)−H(16c)	112.9
O(4)−C(10)−N(1)	111.8(2)	C(15)−C(16)−H(16a)	113.9
O(4)−C(10)−C(11)	125.3(2)	C(15)−C(16)−H(16b)	115.8
N(1)−C(10)−C(11)	123.0(2)	H(16c)−C(16)−H(16a)	95.7
C(10)−C(11)−C(12)	115.3(2)	H(16c)−C(16)−H(16b)	112.8
O(5)−C(12)−N(2)	119.0(2)	H(16a)−C(16)−H(16b)	103.7
O(5)−C(12)−C(11)	117.2(2)	O(6)−C(17)−H(17c)	117.0
N(2)−C(12)−C(11)	123.8(2)	O(6)−C(17)−H(17a)	118.3
N(3)−C(15)−C(6)	115.1(2)	O(6)−C(17)−H(17b)	109.5
N(3)−C(15)−C(16)	124.4(2)	H(17c)−C(17)−H(17a)	89.5
C(6)−C(15)−C(16)	120.5(2)	H(17c)−C(17)−H(17b)	101.8
C(2)−C(3)−H(3)	124.7	H(17a)−C(17)−H(17b)	118.3

and torsion angles of the crystal are listed in Tables 4, 5, and 6, respectively. An ORTEP drawing of **1** with atomic numbering is cited in Figure 4. Figure 5 shows the packing mode in the unit cell for **1** viewed along the *b*-axis.

The torsion angles about O(6)−N(3)−C(15)−C(16) [Table 6; −179.7°] were indicated as the synperiplanar conformation between the methyl group and methoxy group in the iminoxy moiety, which confirmed the configuration of the oxime moiety as *E* form.

Among other moieties, the torsion angles about C(1)−C(2)−O(3)−C(9) and N(2)−C(9)−O(3)−C(2) were indicated as −90.8° and 175.1°, respectively, and the conformations indicated that the plane of the benzene ring was vertical against that of the pyrimidine ring. This conformation is the result of intermolecular repulsion due to the steric hindrance of the ortho-substituted methoxycarbonyl group. The dihedral angle between the plane of the benzene ring and the plane of the iminoxy moiety is 30°.

These findings clearly confirm compound **1** as the *E* form. Thus, KIH-6127 is mainly methyl 2-[(4,6-dimethoxypyrimidin-2-yl)oxy]-6-[1-*E*-(methoxyimino)-ethyl] benzoate (compound **1**).

Stereochemical Aspect of the *E*/*Z* Isomers. The activities of compounds having oximino or imino groups and possibly containing at least two isometric structures (such as *E*/*Z* forms) were of interest. Several examples were tested, and in specific instances we found that either configuration may provide superior biological activity (Hayakawa *et al*., 1991; Matsuura *et al*., 1994). Therefore, the configurational differences between these isomers may determine difference herbicidal activities.

To clarify such different stereochemical behavior, several *Z* isomers were isolated by chromatography and their herbicidal activities measured (Tamaru *et al*., 1997).

These *Z* isomers as well as their corresponding isomers showed high herbicidal activity despite the diversity of their configurations (Table 1). This similarity in activity was unexpected.

To investigate these findings, the physicochemical properties of the *Z* isomers such as log *P* and the soil adsorption coefficient were measured and compared to their corresponding *E* isomers (Table 1). The *Z* isomers show stronger hydrophilic properties and weaker soil adsorption than their counterpart *E* isomers (Table 1).

In the past decade, the computation of the log *P* value from structural information has been pursued by many physical chemists (Hansch and Leo, 1995). The surface area of the molecule (i.e., the water-coated area at which each molecule is covered with a 1.5 Å thick layer representing water) plays an important role as a key factor determining the log *P* value. The surface area of the molecule also determines other structural properties of the molecule (Camilleri *et al*., 1988).

To examine the relationship between log *P* and the diversity of the configuration of the iminoxy moiety, we calculated the whole surface area of both isomers of KIH-6127 as a typical example. The calculated surface area of the *Z* isomer is smaller than that of the *E* isomer as listed in Table 7. It was suggested that the *Z* configuration of the iminoxy moiety contributes to reduce the surface area of the molecule by taking a more compact molecular conformation. Consequently the *Z* isomers become more hydrophilic than the corresponding *E* isomers. The diversity of their configurations merely contributes to the hydrophilicity of the compounds.

Results of QSAR Studies. The fourteen *E* isomers of KIH-6127 derivatives listed in Table 1 were analyzed to examine the quantitative correlation between their structures and herbicidal activity against barnyard grass in pre-emergence. The QSAR analysis gave eq 1 as

$$PI_{50}(\text{pre}) = \underset{(0.084)}{-0.353(\log P)^2} + \underset{(0.505)}{2.151 \log P} + 0.977 \quad (1)$$

Table 6. Torsion Angles (Deg)

atom−atom−atom−atom	angle	atom−atom−atom−atom	angle
O(1)−C(2)−O(2)−C(8)	7.4(4)	N(3)−C(15)−C(6)−C(1)	28.0(3)
O(1)−C(7)−C(1)−C(2)	59.9(3)	N(3)−C(15)−C(6)−C(5)	−149.6(2)
O(1)−C(7)−C(1)−C(6)	−112.9(3)	C(1)−C(2)−O(3)−C(9)	−90.8(2)
O(2)−C(7)−C(1)−C(2)	−116.2(2)	C(1)−C(2)−C(3)−C(4)	1.4(4)
O(2)−C(7)−C(1)−C(6)	61.0(2)	C(1)−C(6)−C(5)−C(4)	−1.4(4)
O(3)−C(2)−C(1)−C(6)	−117.7(2)	C(1)−C(6)−C(15)−C(16)	−152.3(2)
O(3)−C(2)−C(1)−C(7)	−0.4(3)	C(1)−C(7)−O(2)−C(8)	−176.3(2)
O(3)−C(2)−C(3)−C(4)	175.0(2)	C(2)−C(1)−C(6)−C(5)	4.1(3)
O(3)−C(9)−N(1)−C(10)	178.6(2)	C(2)−C(1)−C(6)−C(15)	−173.6(2)
O(3)−C(9)−N(2)−C(12)	−178.8(2)	C(2)−C(3)−C(4)−C(5)	1.4(4)
O(4)−C(10)−N(1)−C(9)	−178.8(2)	C(3)−C(2)−O(3)−C(9)	95.4(3)
O(4)−C(10)−C(11)−C(12)	−179.9(2)	C(3)−C(2)−C(1)−C(6)	−4.2(3)
O(5)−C(12)−N(2)−C(9)	179.9(2)	C(3)−C(2)−C(1)−C(7)	173.1(2)
O(5)−C(12)−C(11)−C(10)	178.9(2)	C(3)−C(4)−C(5)−C(6)	−1.3(4)
O(6)−N(3)−C(15)−C(6)	−179.7(2)	C(4)−C(5)−C(6)−C(15)	176.3(2)
O(6)−N(3)−C(15)−C(16)	0.6(3)	C(5)−C(6)−C(1)−C(7)	−173.1(2)
N(1)−C(9)−O(3)−C(2)	−5.3(3)	C(5)−C(6)−C(15)−C(16)	30.1(3)
N(1)−C(9)−N(2)−C(12)	1.6(3)	C(7)−C(1)−C(6)−C(15)	9.2(3)
N(1)−C(10)−O(4)−C(13)	172.3(2)	C(9)−N(1)−C(10)−C(11)	0.2(3)
N(1)−C(10)−C(11)−C(12)	1.2(3)	C(9)−N(2)−C(12)−C(11)	0.2(3)
N(2)−C(9)−O(3)−C(2)	175.1(2)	C(11)−C(10)−O(4)−C(13)	−6.7(4)
N(2)−C(9)−N(1)−C(10)	−1.8(3)	C(11)−C(12)−O(5)−C(14)	−176.3(2)
N(2)−C(12)−O(5)−C(14)	4.0(3)	C(15)−N(3)−O(6)−C(17)	176.6(3)
N(2)−C(12)−C(11)−C(10)	−1.5(3)		

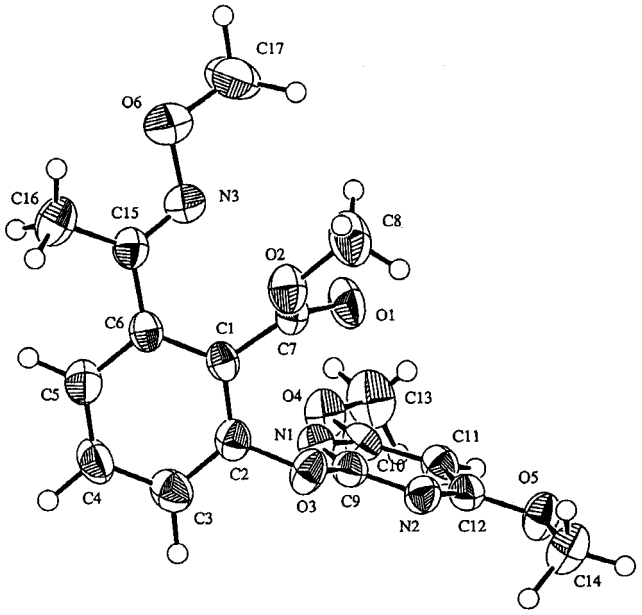

Figure 4. ORTEP drawing of KIH-6127-E (**1**) with atomic numbering.

where $n = 14$, $S = 0.223$, $r = 0.943$, and $F_{2,11} = 44.0$. In this and the following equations, s is the standard deviation, r is the correlation coefficient, and F is the F-test of the correlation with p equal to the number of independent variables in the analysis and q equal to the degrees of freedom ($q = n - p - 1$). The figures in parentheses are the 95% confidence intervals.

Equation 1 shows herbicidal activity to be related parabolically to log P values of the test compounds. The optimal log P value obtained from eq 1 is 3.04. It should be noted that compound **4** (OEt) has the nearest optimum value for log P. As a result, this value is little larger than that of KIH-6127 which we had selected. The equation also suggests that excessively lipophilic or hydrophilic compounds (beyond the range of between 2 and 4 for log P values) should have low pre-emergence herbicidal activity. However, the coefficient of the (log P)^2 term in eq 1 is large, meaning that the effect of changing the log P value on the corresponding herbicidal activity is relatively small.

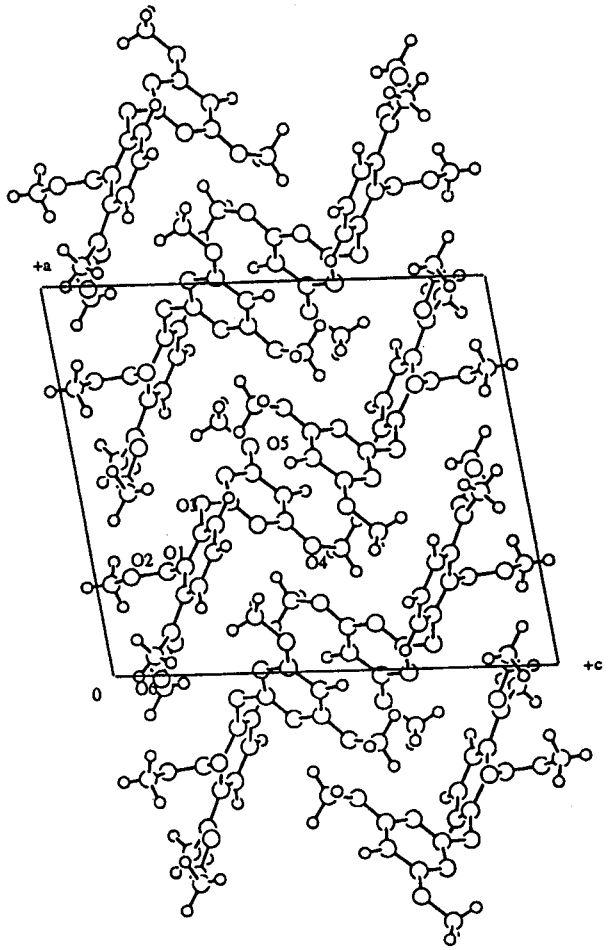

Figure 5. Packing mode in the unit cell for KIH-6127-E (**1**) viewed along the *b*-axis.

We discussed the stereochemical behavior of the configuration in the iminoxy moiety and then carried out a QSAR analysis including the *Z* isomers as shown in eq 2.

$$pI_{50}(\text{pre}) = -0.358(\log P)^2 + 2.193 \log P + 0.884 \quad (2)$$

$$(0.071) \qquad (0.427)$$

Table 7. Calculated Surface Area and Results from the MO Calculation

	E form (compound **1**)	*Z* form (compound **2**)
surface area	343.72 Å^2	329.94 Å^2
final heat of formation (ΔH_f)	194.83 kcal	201.01 kcal
total energy	−4964.87 ev	−4964.60 ev

where $n = 19$, $s = 0.214$, $r = 0.939$, and $F_{2,16} = 59.5$. From the results of both equations, the optimum log P values are 3.05 and 3.06, and the coefficients of the (log P)^2 term are 0.353 and 0.358, respectively. These similarities supported the stability of the equation, even including the Z isomers, and also our discussions about the stereochemical behavior.

Next, further QSAR analysis was done using pI_{50}(post) of the herbicidal activity against barnyard grass at the three-leaf growth stage to obtain eq 3 as

$$\mathrm{p}I_{50}(\mathrm{post}) = -0.419(\log P)^2 + 2.262 \log P + 0.743 \quad (3)$$
$$(0.103) \qquad (0.599)$$

where $n = 15$, $s = 0.252$, $r = 0.943$, and $F_{2,12} = 48.2$. Similarly to eq 2, eq 3 shows herbicidal activity to be related to the square of the log P values of the compounds. The optimal log P value obtained from eq 3 was 2.69 and smaller than that of eq 2. This suggested that a more hydrophilic compound is desirable for herbicidal activity against barnyard grass at the three-leaf growth stage rather than at pre-emergence application.

Because the coefficients of the (log P)^2 terms in eqs 1−3 are relatively large compared to log P coefficients, the effects of changing log P on herbicidal activity are rather small.

In Table 1, the deviation between the minimum activity of pre-emergence and the maximum phytotoxicity is 1.78 [$\Delta \mathrm{p}I_{50} = \mathrm{p}I_{50}(\mathrm{pre})_{\min} - \mathrm{p}I_{50}(\mathrm{rice})_{\max} = 3.65 - 1.87$]. The derivatives listed here show a selectivity greater than 10 times for barnyard grass over rice. The QSAR of the phytotoxicity against rice was carried out. Finally eq 4 was obtained after the preliminary analysis as

$$\mathrm{p}I_{50}(\mathrm{rice}) = -0.366K_d + 2.164 \quad (4)$$
$$(0.121)$$

where $n = 12$, $s = 0.156$, $r = 0.906$, and $F_{1,10} = 45.4$. In eq 4, the soil adsorption coefficient K_d is taken as a fixed parameter. The phytotoxicity toward rice is inversely proportional to the K_d value.

Compound **1** was selected as the candidate for commercialization as a novel barnyard grass herbicide with a characteristics well balanced for pre-emergence activity, high-leaf growth stage activity, and acceptable safety.

ACKNOWLEDGMENT

We express our thanks to Professor Nobuo Tanaka, Tokyo Institute of Technology, for his X-ray crystallographic experiments and many helpful suggestions for the results and manuscript.

LITERATURE CITED

Camilleri, P.; Watts, S.; Boraston, J. A Surface Area Approach to Determination of Partition Coefficients. *J. Chem. Soc., Perkin Trans. 2*, **1988**, 1699−1707.

Dewar, M. J. S.; Zoebish, E. G.; Hearly, E. F.; Stewart, J. J. AM 1: A New General Purpose Quantum Mechanical Molecular Mode. *J. Am. Chem. Soc.* **1985**, *107*, 3902−3909.

Fujita, T.; Iwasa, J.; Hansch, C. A New Substituent Constant, *p*, Derived from Partition Coefficients. *J. Am. Chem. Soc.* **1964**, *86*, 5175−5179.

Hanai, R.; Kawano, K.; Shigematsu, S.; Tamaru, M. KIH-6127, A New Selective Herbicide to Control Barnyard grass in Rice. *Proc. Brighton Crop. Prot. Conf.—Weeds* **1993**, *1*, 47−52.

Hansch, C.; Leo, A. *Exploring QSAR: Fundamentals and Applications in Chemistry and Biology*; Hansch, C., Leo, A., Eds.; ACS Professional Reference Book Series; American Chemical Society: Washington, DC, 1995; Vol. 1, pp 105−111.

Hayakawa, K.; Nakayama, A.; Nishikawa, H.; Nakata, A.; Sato, S.; Yokata, C. Fungicidal Properties of *N*-(3,5-Dichlorophenyl)-*N*′-methoxyformamidine and Computer Studies of Its Active Structures. *Nihon Noyaku Gakkaishi (J. Pestic. Sci.)* **1991**, *16*, 481−490.

Lambert, S. M.; Omega (Ω), a Useful Index of Soil Sorption Equilibria. *J. Agric. Food Chem.* **1968**, *16*, 340−343.

Main, P.; Hull, S. E.; Lessinger, L.; Germain, G.; Declereg, J. P.; Woolfson, M. M. *MULTAN 78: A System of Computer Programs for the Automatic Solution of Crystal Structures from X-ray Diffraction Data*; Universities of York, England, and Louvain, Belgium, 1978.

Matsuura, K.; Ishida, Y.; Kuragano, T.; Konishi, K. Development of a New Fungicide, Ferimzone. *Nihon Noyaku Gakkaishi (J. Pestic. Sci.)* **1994**, *19*, 325−327.

OECD Guidelines for Testing of Chemicals; No. 117, adopted by the Council on March 30, 1989.

Shimizu, T.; Nakayama, I.; Nakano, T.; Nezu, Y.; Abe, H. Inhibition of Plant Acetolactate Synthase by Herbicides, Pyrimidinyl Salicyclic Acids. *Nihon Noyaku Gakkaishi (J. Pestic. Sci.)* **1994**, *19*, 59−67.

Shimizu, T.; Nakayama, I.; Nakao, T.; Takahashi, S.; Tamaru, M.; Wada, N.; Abe, H. *Int. Cong. Pestic. Chem., 8th*, **1994**, *9B*, 669.

Takahashi, Y.; Hosokawa, K.; Yoshida, F.; Ozaki, M.; Sasaki, S.; A New System, TU-TORS, for Computer-Aided Molecular Design. *Anal. Chim. Acta* **1989**, *217*, 61−83.

Tamaru, M.; Saito, Y. Studies of the New Herbicide KIH-6127. Part I. Novel Synthesis of Methyl 6-Acetylsalicylates as a Key Synthetic Intermediate for Preparation of 6-Acetyl Pyrimidin-2-yl Salicylates and Analogues. *Pestic. Sci.* **1996**, *47*, 125−130.

Tamaru, M.; Takehi, T.; Masuyama, N.; Hanai, R. Studies of the New Herbicide KIH-6127. Part II. Synthesis and Herbicidal Activity of 6-Acyl Pyrimidin-2-yl Salicylates and Analogues against Barnyard Grass. *Pestic. Sci.* **1996**, *47*, 327−335.

Tamaru, M.; Masuyama, N.; Sato, M.; Takabe, F.; Inoue J. Studies of the New Herbicide KIH-6127. Part III. Synthesis and Structure−Activity studies of Analogues of KIH-6127 Against Barnyard Grass. *Pestic. Sci.* **1996**, *49*, 76−84.

Received for review November 5, 1996. Accepted March 28, 1997.[⊗]

JF960844V

[⊗] Abstract published in *Advance ACS Abstracts*, June 15, 1997.